BULLETIN OF THE EARTHQUAKE
RESEARCH INSTITUTE
Vol. 44 (1966), pp. 1553-1570

75. *Electrical Conductivity of Strained Rocks. The Second Paper. Further Experiments on Sedimentary Rocks.*

By Yoshio YAMAZAKI,

Earthquake Research Institute.

(Read Sept. 27, 1966.—Received Sept. 30, 1966.)

Summary

Changes in the resistivity of three kinds of sedimentary rocks, lapilli tuff, tuffaceous sandstone and pumice tuff, are studied in fair detail by making use of an oil pressure testing machine. The rate of change in resistivity for a lapilli tuff sample from Aburatsubo proved to be extremely large amounting to a value a few hundred times as large as the change in mechanical strain, the results generally confirming those preliminarily obtained in the previous paper. Although a simple theory of electric conduction in a strained rock containing water is advanced in Appendix, no good agreement between the theory and actual experiments was obtained.

1. Introduction

It has been studied in the first report[1] that resistivity of sedimentary rocks changes when the rock specimens are strained. It has also been found that a particular rock sample, the lapilli tuff from Aburatsubo, exhibits an extremely large rate of change in the resistivity, $10^2 \sim 10^3$ times as large as the mechanical strain.

The experiments in the previous paper should be regarded, however, as preliminary because rock specimens were strained by a crude device. It was difficult to strain them continuously. The loading technique was so poor that the writer sometimes worried about non-uniformity of strain.

It is therefore intended in this paper to report on the relationship between changes in resistivity and those in strain on the basis of a series of more refined experiments. A simple oil pressure compression testing machine is specially made for the experiments as will be seen in Section 2. Section 3 will be reserved for briefly outlining the method

1) Y. YAMAZAKI, *Bull. Earthq. Res. Inst.*, **43** (1965), 783-802.

of measuring changes in resistivity of a rock specimen. Rate of change in the resistivity of lapilli tuff from Aburatsubo as revealed by the experiments will be reported in fair detail in Section 4 which will be followed by similar results for other rock samples in Section 5. Porosities, permeabilities and the like of the samples studied will be reported in Section 6 together with discussion of the experimental results. A theory on electrical conductivity of strained rocks containing water will be advanced in Appendix.

2. Oil pressure compression testing machine

An oil pressure compression testing machine as can be seen in Fig. 1 is used throughout the present experimental work. On rotating the

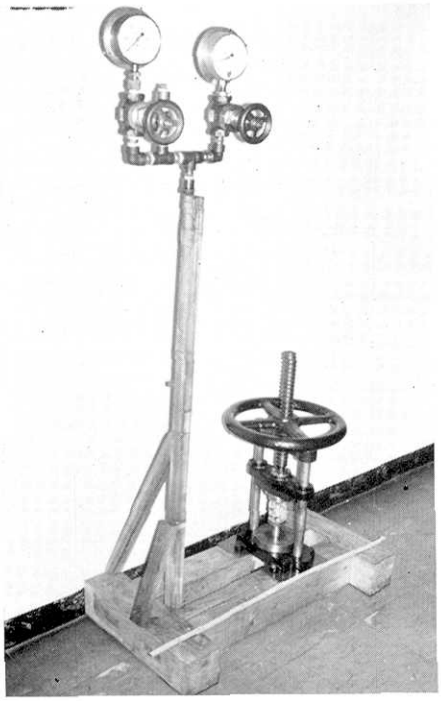

Fig. 1. Oil pressure compression testing machine.

wheel, pressures up to 150 kg/cm^2 at maximum can be produced between the two iron platens, insulated with one another. The diameter of the platens amounts to 6 cm. Two pressure gauges are used for ranges 0~10 kg/cm^2 and 0~150 kg/cm^2 respectively. As for the specimens for

the compression tests, rock samples are shaped in either $40\times40\times65$ mm or $35\times36\times65$ mm prisms. Strain gauge elements are attached to rock specimens in a similar fashion as reported in the first paper. Changes in strain are amplified and recorded by a pen-writing recorder.

3. Bridge method for measuring small changes in resistivity of rock specimen

A rock specimen, to which ends are attached copper electrodes, is inserted in one of the branches of a bridge circuit which is schematically shown in Fig. 2. The circuit is about the same as that described in the

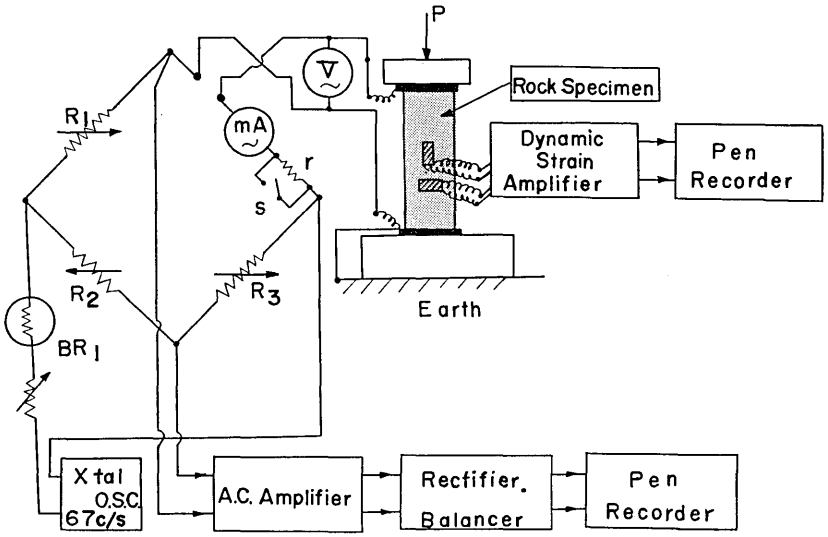

Fig. 2. Schematic diagram of the compression experiment by a bridge method.

first paper. An important improvement is the use of a 67 c.p.s. oscillator in place of a generator driven by a synchronous motor. The oscillator bases on a quartz crystal with frequency and voltage accuracies of 10^{-5} and 10^{-4} respectively. The maximum output current is 150 mA at 450 V. Fluctuations in the voltage and frequency that were the main source of error in the previous experiments are considerably reduced by introducing the present oscillator. The frequency is deliberately chosen at 67 c.p.s. so as to be incommensurable to the 50 or 60 c.p.s. in order to minimize possible contamination by the commercial alternating current.

An equivalent circuit of the bridge is shown in Fig. 3. On condition that the additional resistance r is negligibly smaller than R_1, R_2, R_3

and R_x, the voltage between c and d is given by

$$v_{cd}=i_g R_g=\frac{R_x R_2-R_1 R_3}{(R_1+R_x)(R_2+R_3)}E_0\,, \quad (1)$$

provided R_g is very much larger than R_1, R_2, R_3 and R_x.

The balance of the bridge circuit is therefore achieved when

$$R_x=R_1R_3/R_2\,. \quad (2)$$

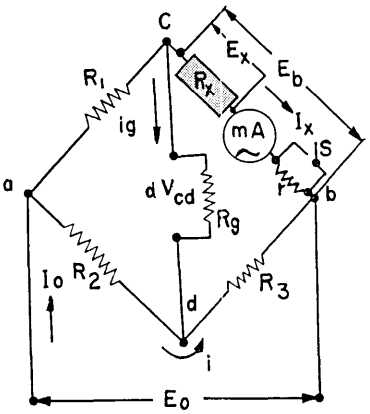

Fig. 3. Equivalent circuit of the bridge method.

After balancing is established, R_x is assumed to change by a small amount dR_x because of mechanical strain of the rock specimen. In that case v_{cd} changes by a small amount dv_{cd} which is readily obtained from (1) as

$$dv_{cd}=\frac{E_0R_1}{(R_1+R_x)^2}dR_x\,, \quad (3)$$

so that, if dv_{cd} is actually measured, dR_x can be calculated according to a formula

$$dR_x=\frac{(R_1+R_x)^2}{E_0R_1}dv_{cd}\,, \quad (4)$$

in which R_1, R_x and E_0 are all measurable.

An alternative way of determining the sensitivity on the recording paper is effected in the following way. The pen of the recorder displaces by an amount D mm when the resistance r for calibration is shunted by switch S after balancing. In that case the change in the resistivity which is required for 1 mm deflection of the pen is obtained as $\frac{r}{R_B}\frac{1}{D}$, where R_B is the resistance between b and c, R_B being approximately equal to R_x. It has been proved that both the methods of determining the sensitivity lead to good agreement. As the resistivity is given by

$$\rho=RA/L\,, \quad (5)$$

where R is the resistance, A the cross-section area and L the length of the rock specimen, the rate of change in the resistivity is estimated by

$$\Delta\rho/\rho=\Delta R/R-(1-2\sigma)\Delta L/L\,, \quad (6)$$

where σ denotes *Poisson's* ratio. (6) has been already given in the first report.

4. Experiments on lapilli tuff specimens from Aburatsubo

Fig. 4 shows the changes in the resistivity of a lapilli tuff specimen, which is so dry that the water content is estimated as 2 per cent and the resistivity at unstrained state amounts to $6.9\times10^{4}\,\Omega$-cm, by the compression test. The electric current flowing through the specimen is 6 mA. Simultaneous measurements of strain make it possible to draw a $\Delta\rho/\rho - \Delta L/L$ diagram as shown in Fig. 5. In this case the rate of change in the resistivity is linearly correlated with the change in strain. The mean ratio $\frac{\Delta\rho}{\rho}/\frac{\Delta L}{L}$ is estimated as 400.

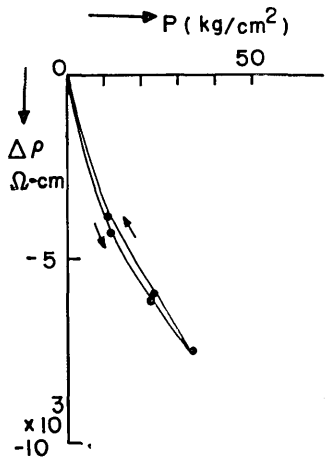

Fig. 4. Changes in the resistivity by compression of a lapilli tuff specimen from Aburatsubo. The water content in weight is estimated as 2 per cent.

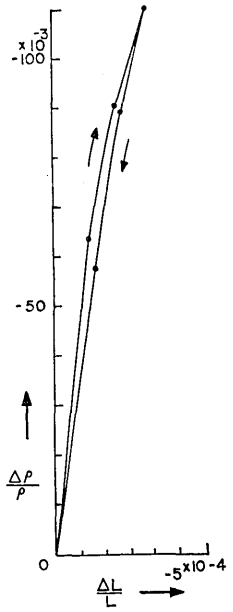

Fig. 5. $\Delta\rho/\rho$ versus $\Delta L/L$ relation of the lapilli tuff specimen at a water content of 2 per cent.

The resistivity of this particular specimen greatly decreases by adding water. The resistivity at a water content 18 per cent becomes only $9.7\times10^{2}\,\Omega$-cm. Similar experiments on the specimen under such a condition indicate that the resistivity change behaves against the strain change

as shown in Fig. 6, the mean $\frac{\Delta\rho}{\rho}/\frac{\Delta L}{L}$ being estimated as 250 at an electric current intensity 7 mA. As the water content increases, the specimen begins to behave anelastically, so that $\frac{\Delta\rho}{\rho}-\frac{\Delta L}{L}$ relations for loading and unloading processes do not coincide.

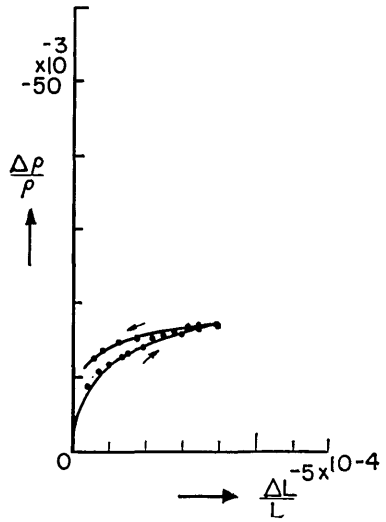

Fig. 6. $\Delta\rho/\rho$ versus $\Delta L/L$ relation of the lapilli tuff specimen at a water content of 18 per cent.

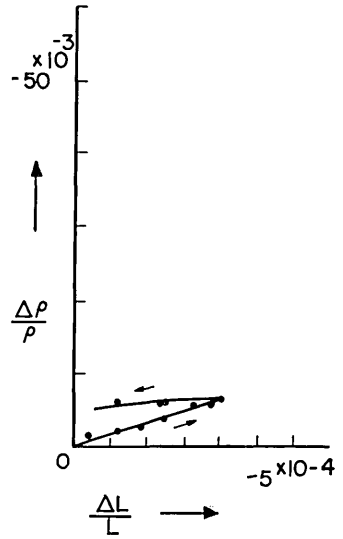

Fig. 7. $\Delta\rho/\rho$ versus $\Delta L/L$ relation of the lapilli tuff specimen at a water content of 25 per cent.

The irreversibility of $\frac{\Delta\rho}{\rho}-\frac{\Delta L}{L}$ curve becomes more outstanding at a water content 25 per cent at which the resistivity amounts to only $6.4\times10^{2}\,\Omega$-cm. As can be seen in Fig. 7 the discrepancy between the loading and unloading processes is so large that only the loading curve may be used for estimating the mean $\frac{\Delta\rho}{\rho}/\frac{\Delta L}{L}$. The ratio amounts to only 25 in this case for a current intensity 7 mA.

It has been noticed throughout the present experiments that $\Delta\rho$ tends to saturate for a large $\Delta L/L$, so that individual $\frac{\Delta\rho}{\rho}/\frac{\Delta L}{L}$ for a small $\Delta L/L$ is larger than that for a large $\Delta L/L$. Fig. 8 indicates how $\frac{\Delta\rho}{\rho}/\frac{\Delta L}{L}$ changes with $\Delta L/L$ for a moderately wet (water content: 18 percent) specimen. All the results for a range of applied electric current

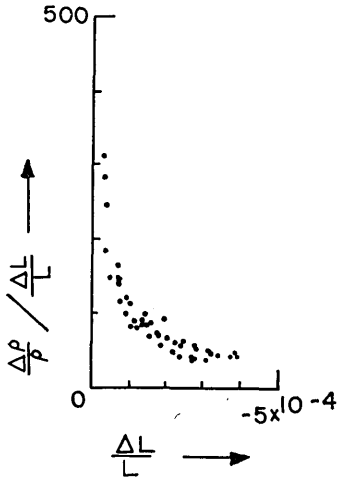

Fig. 8. Individual values of $\frac{\Delta\rho}{\rho} / \frac{\Delta L}{L}$ of the lapilli tuff specimen (water content: 18 per cent) plotted against $\Delta L/L$.

from 4 to 8 mA are plotted in the figure. As will be shown later, $\frac{\Delta\rho}{\rho} / \frac{\Delta L}{L}$ is almost constant for any $\Delta L/L$ for the other specimens of different rock types, say taffaceous sandstone from Aburatsubo and pumice tuff from Oya. Such a difference seems to reflect the different mechanism of electric conduction between what the writer called the A-type and O-type rocks in the previous paper.

Relation (6) in fact leads to

$$\frac{\Delta\rho}{\rho} / \frac{\Delta L}{L} = \frac{\Delta R}{\Delta L} / \frac{R}{L} - 1 + 2\sigma \,, \qquad (7)$$

from which we see that $\frac{\Delta\rho}{\rho} / \frac{\Delta L}{L}$ is a constant provided ΔR is proportional to ΔL. For an O-type rock, we may assume that the proportionality holds good, so that $\frac{\Delta\rho}{\rho} / \frac{\Delta L}{L}$ is constant for the tuffaceous sandstone and pumice tuff experimented. On the other hand, $\Delta R/\Delta L$ is larger for a small ΔL than that for a large ΔL in the case of the lapilli tuff which was defined as one of the A-type rocks.

It was stated in the previous paper that there is a tendency that $\frac{\Delta\rho}{\rho} / \frac{\Delta L}{L}$ tends to take a larger value when the sample is wet. According to the present series of experiments, such a conclusion is not correct. Probably the false conclusion was drawn because only a few tests, which did not cover a wide range of strain, were conducted.

It is of interest and importance that $\frac{\Delta\rho}{\rho} / \frac{\Delta L}{L}$ which exceeds a few hundred is obtained even in the present experiments on the lapilli tuff from Aburatsubo for a strain amounting to 10^{-4} or smaller. The results are compatible with those reported in the previous paper.

5. Experiments on tuffaceous sandstone from Aburatsubo and pumice tuff from Oya

Experiments similar to those in the last section are made for two

kinds of rock specimen. One is a tuffaceous sandstone taken from almost the same place at Aburatsubo where the lapilli tuff studied in the last section was sampled and the other a pumice tuff from Oya, Tochigi Prefecture. As it is tedious to describe all the experimental results, only two examples of $\Delta\rho/\rho$ versus $\Delta L/L$ relations are shown in Figs. 9 and 10 respectively for tuffaceous sandstone and pumice tuff. In both cases, the electric current used is 8 mA, while the water contents are 9.5 and 5.6 percent respectively.

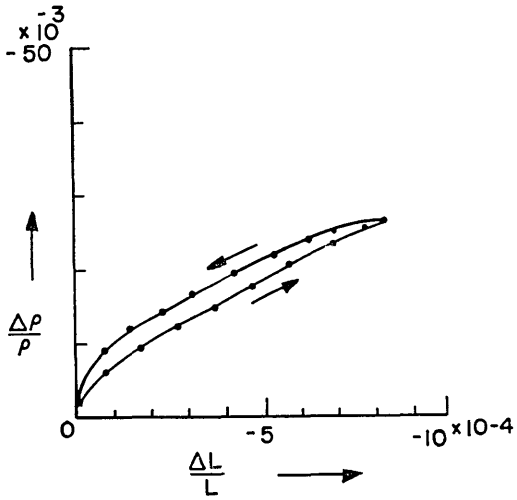

Fig. 9. $\Delta\rho/\rho$ versus $\Delta L/L$ relation of a tuffaceous sandstone from Aburatsubo at a water content of 9.5 per cent.

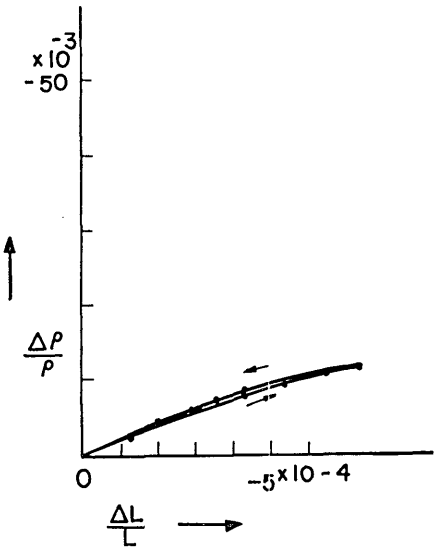

Fig. 10. $\Delta\rho/\rho$ versus $\Delta L/L$ relation of a pumice tuff from Oya at a water content of 5.6 per cent.

It is seen in these figures that $\Delta\rho/\rho$ is considerably smaller than that for the lapilli tuff, mean $\frac{\Delta\rho}{\rho}/\frac{\Delta L}{L}$ being estimated as 30 and 18 respectively.

All the values of $\frac{\Delta\rho}{\rho}/\frac{\Delta L}{L}$ for a range of electric current from 6 to 8 mA are plotted against $\Delta L/L$ as can be seen in Figs. 11 and 12 respectively for the tuffaceous sandstone at water content 9.5 percent and the pumice tuff at 5.6 percent. Unlike the case of the lapilli tuff as shown in Fig. 8, no marked dependence of $\frac{\Delta\rho}{\rho}/\frac{\Delta L}{L}$ on $\Delta L/L$ can be found.

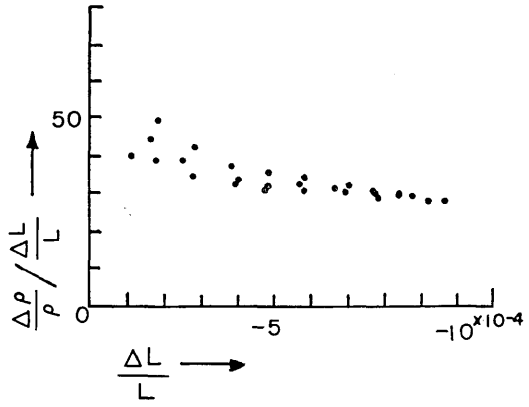

Fig. 11. Individual values of $\frac{\Delta\rho}{\rho} / \frac{\Delta L}{L}$ of the tuffaceous sandstone (water content: 9.5 per cent) plotted against $\Delta L/L$.

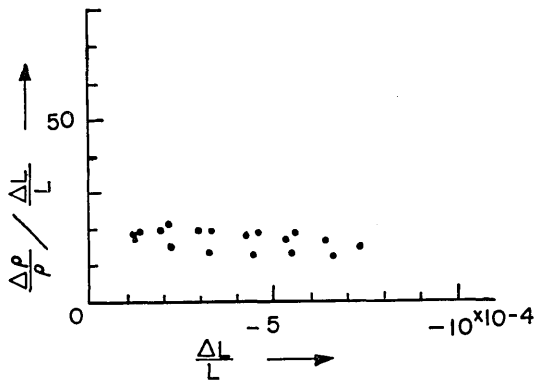

Fig. 12. Individual values of $\frac{\Delta\rho}{\rho} / \frac{\Delta L}{L}$ of the pumice tuff (water content: 5.6 per cent) plotted against $\Delta L/L$.

6. Discussion

What the writer has been dealing with in the foregoing sections strongly indicates the fact that the mechanism of electric conduction for the lapilli tuff (A-type) is different from that for the tuffaceous sandstone and pumice tuff (O-type). The anomalous feature of an A-type rock specimen which has been pointed out in the previous paper is here confirmed again.

In the hope of getting some idea about the difference between the conduction mechanisms of A-type and O-type rocks, porosities, permeabilities

and the like are measured for typical specimens[2]. In Table 1 are shown the results of the measurements.

Table 1. Porosities, permeabilities and other elements of three rock specimens.

Specimen	Lapilli tuff	Tuffaceous sandstone	Pumice tuff
Rock type	A	O	O
Bulk density	1.69 g/cm³	1.84 g/cm³	1.74 g/cm³
Specific gravity	2.49	2.87	2.26
Water content	32.1%	22.6%	23.1%
Void ratio	1.17	1.02	0.69
Porosity[3]	40.8%	51.4%	56.7%
Permeability[4]	3.6 md	0.013 md	0.062 md

It is noticeable that the permeability of the lapilli tuff specimen is far larger than those of the other specimens although the porosity is a little smaller. Permeability is the only quantity which indicates a large contrast among the quantities shown in Table 1. It seems to the writer that the fact is very important in discussing the possible mechanism of electric conduction. A model, in which overlapped spherical holes filled with conducting water as discussed in the first paper, could be supported by the high value of permeability of the A-type rock specimen.

Resistivity (ρ) versus water content (w) curves for the three specimens are also drawn on the basis of experiments on disk samples of 2.5 cm in diameter and 2 cm in thickness. An electric furnace at moderate temperature is made use of for drying up the samples. As shown in Fig. 13, the curves for tuffaceous sandstone and pumice tuff are similar in shape, while the curve for the lapilli tuff seems somewhat different from the others. It seems unlikely, however, that even the $\rho-w$ relations for the O-type rocks, the tuffaceous sandstone and the pumice tuff say, could be accounted for by a simple theory developed in Appendix even though a number of likely parameters are chosen. It also turns out by the theory that $\frac{\Delta\rho}{\rho}/\frac{\Delta L}{L}$ may take widely different values, either plus

2) Actual measurements are made by Dr. H. ARAKI.

3) Porosities are measured by an air diffusion method for samples at a temperature range from 105 to 110°C.

4) Permeabilities are measured at a mean pressure of 1 atmosphere and at a temperature of 20°C. When 1 cm³ water passes through 1×1×1 cm cube specimen during 1 second under a pressure difference of 1 atmosphere, the permeability is defined as 1 darcy.

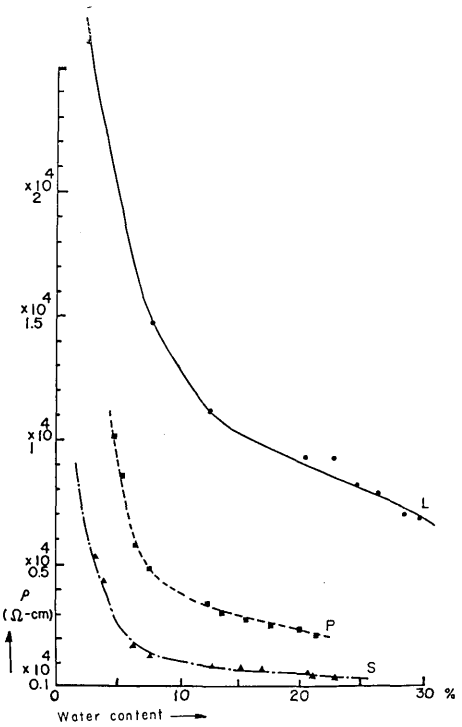

Fig. 13. Changes in the resistivity of the three samples with the water content. *L*: Lapilli tuff from Aburatsubo, *S*: Tuffaceous sandstone from Aburatsubo, *P*: Pumice tuff from Oya.

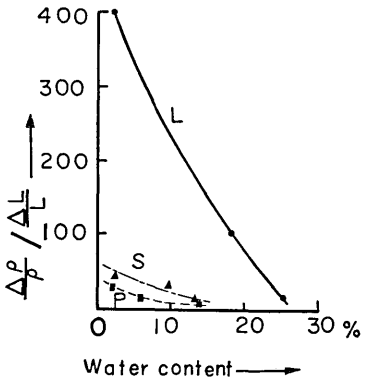

Fig. 14. $\frac{\Delta\rho}{\rho} / \frac{\Delta L}{L}$ values at $\Delta L/L = 10^{-4}$ for the three rock samples, as described in the caption of Fig. 13, plotted against water content.

or minus, according to different combinations of the parameters. The writer thinks, therefore, that the mechanism of electric conduction of the sedimentary rocks, either the A-type or the O-type, should be discussed on the basis of a much more sophisticated model than that given in Appendix although the writer has no concrete idea about a better model.

Fig. 14 shows the $\frac{\Delta\rho}{\rho} / \frac{\Delta L}{L}$ versus water content relations of the three rock samples at $\Delta L/L=10^{-4}$. The great contrast between the $\frac{\Delta\rho}{\rho} / \frac{\Delta L}{L}$ values for the lapilli tuff and those for the other two rock samples is clearly demonstrated at all the water contents.

7. Conclusion

As a result of a series of compression experiments on three kinds of sedimentary rock specimens, lapilli tuff, tuffaceous sandstone and pumice tuff, it is made clear that the rate of resistivity change of the lapilli tuff from Aburatsubo takes on a very large value, say a few hundred times as large as the change in strain, especially for a small strain, 10^{-4} or less.

Meanwhile the rates of resistivity change for a tuffaceous sandstone sample from Aburatsubo and a pumice tuff specimen from Oya do not take on such a large value. They are of the same order as the changes in mechanical strain or a little larger. The results generally agree with those already reported in the writer's first paper.

As the permeability of the lapilli tuff is extremely larger than those of the other samples, it is surmised that the anomalous behaviour of electric conduction of the lapilli tuff may have something to do with a special way of water arrangement peculiar to the sample. Although the mechanism of electric conduction in such a type of rock is not clear, a model of slightly overlapped sphere filled with water as suggested in the previous report could be a possible one. A classification as made in the previous paper, A-type for the lapilli tuff and O-type for the other two samples, seems to be adequate.

A simple theory on electric conduction of rocks containing water as will be advanced in Appendix does not lead to a success even for an O-type rock. The actual mechanism of electric conduction in sedimentary rocks must be so complicated that a more elaborate theory is needed in order to reach a better understanding.

Since the rate of resistivity change amounts to a value a few hundred

times as large as that of mechanical strain, however, it seems worthwhile conducting a field measurement of detecting an extremely small change in strain by measuring changes in the resistivity in situ.

In conclusion, the writer wishes to express his sincere thanks to Professor T. Rikitake for his interest and advice in the course of the present work. The computer program for the theory advanced in Appendix was provided by Mr. T. Watanabe to whom the writer is also grateful. A part of the expenses of the present work was defrayed from a grant given to Professor Rikitake by the Ministry of Education.

Appendix: Theory on electrical conductivity of strained rocks containing water

The electrical conductivity in bulk of a medium (conductivity: σ_1) containing spherical conductors (conductivity: σ_2) has been obtained as[5]

$$\sigma_0=\sigma_1\frac{3\sigma_2-v(\sigma_2-\sigma_1)}{3\sigma_1+v(\sigma_2-\sigma_1)}\,, \tag{A-1}$$

where v is the volume content of the latter material. Mutual interaction between the spherical conductors is ignored in obtaining (A-1).

In a theory of thermal conductivity of wet rocks, Horai and Uyeda[6] extended relation (A-1) to a mixture of solid, water and air. The following is more or less along their line.

Let us first think of a completely dry rock which may be idealized by solid particles placed in air as schematically shown in (a) diagram of Fig. 15. In such a case, (A-1) can be written as

$$\sigma_D=\sigma_a\frac{3\sigma_s-2p(\sigma_s-\sigma_a)}{3\sigma_a+p(\sigma_s-\sigma_a)}\,, \tag{A-2}$$

where σ_s and σ_a are respectively the conductivities of solid and air while p is identified as the porosity.

In a similar fashion, the conductivity of completely wet rock which is shown in (b) diagram of Fig. 15 can be written as

$$\sigma_W=\sigma_w\frac{3\sigma_s-2p(\sigma_s-\sigma_w)}{3\sigma_w+p(\sigma_s-\sigma_w)}\,, \tag{A-3}$$

where σ_w is the conductivity of water.

5) J. C. MAXWELL, *A Treatise on Electricity and Magnetism*. 3rd. ii, **1** (1904). Oxford.
6) K. HORAI and S. UYEDA, *Bull. Earthq. Res. Inst.*, **38** (1960), 199-206.

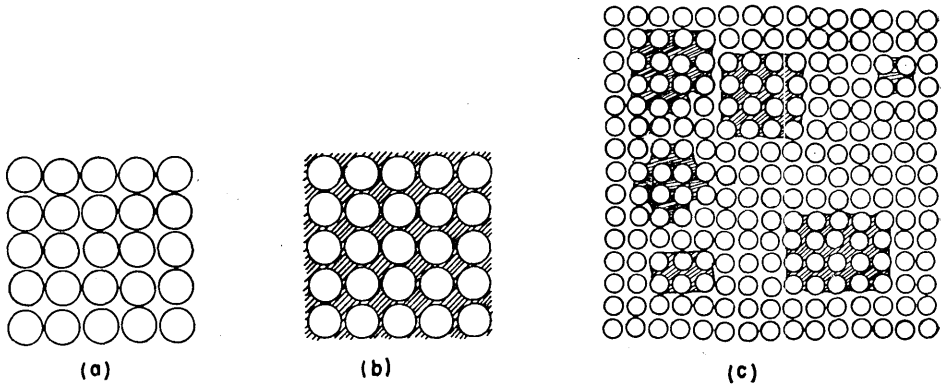

Fig. 15. Schematic representation of the model. (a) Completely dry state, giving σ_D for electric conductivity. Circles represent the solid particles. (b) Saturated state, giving σ_W for conductivity. Hatched part represents the water-filled space. (c) Intermediate state in an undersaturated state.

For an intermediate state between the above two states, we may think of scattered small masses of completely wet state in a completely dry material as can be seen in (c) diagram of Fig. 15. It is therefore possible to get at the conductivity in bulk of such a material by repeating the same idea. We obtain

$$\sigma_A=\sigma_D\frac{3\sigma_W-2(1-v')(\sigma_W-\sigma_D)}{3\sigma_D+(1-v')(\sigma_W-\sigma_D)}\,, \tag{A-4}$$

where $1-v'$ is the the volume ratio of the air contained to the interstitial space in the specimen.

If we denote the volumes of air, water and solid by V_a, V_w and V_s, v' is given by

$$v'=\frac{V_w}{V_a+V_w}\,. \tag{A-5}$$

Meanwhile the porosity is defined by

$$p=\frac{V_w+V_a}{V_s+V_w+V_a}\,, \tag{A-6}$$

so that we obtain

$$v'=\frac{1}{p}\,\frac{V_w}{V_s+V_w+V_a}\,. \tag{A-7}$$

On the other hand, the bulk density and the water content in weight

are respectively defined by

$$D=\frac{D_s V_s+D_w V_w+D_a V_a}{V_s+V_w+V_a}\ , \tag{A-8}$$

$$w=\frac{D_w V_w}{D_s V_s+D_w V_w+D_a V_a}\ , \tag{A-9}$$

where D_s, D_w and D_a are respectively the densities of solid, water and air.

From (A-8) and (A-9), we are led to

$$Dw=\frac{D_w V_w}{V_s+V_w+V_a}\ . \tag{A-10}$$

(A-7) combined with (A-10) lead to

$$v'=\frac{Dw}{pD_w}\ . \tag{A-11}$$

If we ignore $D_a V_a$ in (A-8), we obtain

$$D=D_s(1-p)+Dw\ ,$$

solving which the bulk density becomes

$$D=D_s\frac{1-p}{1-w}\ . \tag{A-12}$$

It is hence possible to estimate conductivity in bulk σ_A provided σ_s, σ_a, σ_w, p, D_s, D_w and w are known. Examples of change in $\rho(=1/\sigma_A)$ with w are calculated as shown in Fig. 16 on the assumption that $D_w=1\,\mathrm{g/cm^3}$, $D_s=2.5\,\mathrm{g/cm^3}$, and $p=0.5$. σ_a, σ_S and σ_w are chosen as are mentioned in the captions. The present theory can only be applied to a range of water content from zero to w_0 which is the water content at the saturation state. w_0 amounts to 28.6 percent in the above model. At that state, the volume of water is correlated to the total weight by

$$w_0=\frac{D_w V_w}{D_s V_s+D_w V_w}\ , \tag{A-13}$$

so that it is obvious that

$$w_0=\frac{p}{p+(1-p)\dfrac{D_s}{D_w}}\ . \tag{A-14}$$

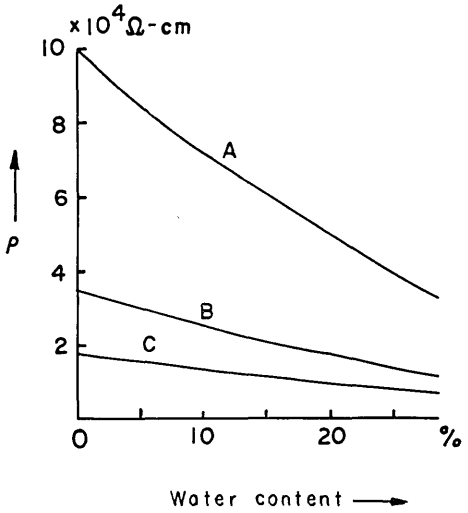

Fig. 16. Changes in ρ with water content for three models. $D_w=1$ g/cm^3, $D_s=2.5$ g/cm^3 and $p=0.5$ are assumed for all the models. The other parameters are as follows. A: $\sigma_s=10^{-5}$, $\sigma_a=10^{-5}$ and $\sigma_w=10^{-2}$. B: $\sigma_s=10^{-4}$, $\sigma_a=10^{-5}$ and $\sigma_w=10^{-2}$. C: $\sigma_s=10^{-4}$, $\sigma_w=2\times10^{-3}$ and $\sigma_a=3\times10^{-5}$. (Unit: ohm^{-1} cm^{-1}).

We are now in a position to estimate the rate of change in the conductivity when rocks as represented by the present model are subjected to a volume change. Differentiating (A-4) with respect to v, we obtain

$$\frac{d\sigma_A}{\sigma_A}=\frac{d\sigma_D}{\sigma_D}+\frac{\frac{\sigma_D}{\sigma_A}\Phi dV}{[3+(1-v')(\xi-1)]^2}\,, \tag{A-15}$$

where

$$\begin{aligned}\Phi dV=&[3+(1-v')(\xi-1)]\\&\times\left[3\xi\frac{d\sigma_W}{\sigma_W}-2\phi\frac{1-2p}{p^2}(\xi-1)\frac{dV}{V}-(1-v')\left(\xi\frac{d\sigma_W}{\sigma_W}-\frac{d\sigma_D}{\sigma_D}\right)\right]\\&-[3\xi-2(1-v')(\xi-1)]\\&\times\left[3\frac{d\sigma_D}{\sigma_D}+\phi\frac{1-2p}{p^2}(\xi-1)\frac{dV}{V}+(1-v')\left(\xi\frac{d\sigma_W}{\sigma_W}-\frac{d\sigma_D}{\sigma_D}\right)\right],\end{aligned} \tag{A-16}$$

$$\frac{d\sigma_D}{\sigma_D}=-\frac{dV}{V}(1-p)\gamma(\alpha-1)\frac{3(\alpha+2)}{[3+p(\alpha-1)]^2}\,, \tag{A-17}$$

$$\frac{d\sigma_W}{\sigma_W}=-\frac{dV}{V}(1-p)\delta(\beta-1)\frac{3(\beta+2)}{[3+p(\beta-1)]^2}\,, \tag{A-18}$$

$$\xi=\frac{\sigma_W}{\sigma_D}\,,\quad \alpha=\frac{\sigma_s}{\sigma_a}\,,\quad \beta=\frac{\sigma_s}{\sigma_w}\,,\quad \gamma=\frac{\sigma_a}{\sigma_D}\,,\quad \delta=\frac{\sigma_w}{\sigma_W}\,,\quad \phi=\frac{wD}{D_w}\,. \tag{A-19}$$

In deducing the relations from (A-15) (A-18), we made use of the following relations:

$$\frac{dp}{dV}=\frac{1-p}{V}\,, \tag{A-20}$$

$$\frac{dv'}{dV}=-\frac{\phi}{V}\frac{1-2p}{p^2}\,, \tag{A-21}$$

where V is the volume of a rock specimen. (A-20) is obtained on the assumption that V_s never changes. As the rate of volume change for a compression test is correlated to linear strain by

$$\frac{dV}{V}=(1-2\sigma)\frac{dL}{L}\,, \tag{A-22}$$

where σ is Poisson's ratio and L a typical length, the relationship between rate of change in the electrical conductivity and linear strain is readily obtained. Examples of $\frac{d\rho}{\rho}$ versus $\frac{dL}{L}$ curve based on the same para-

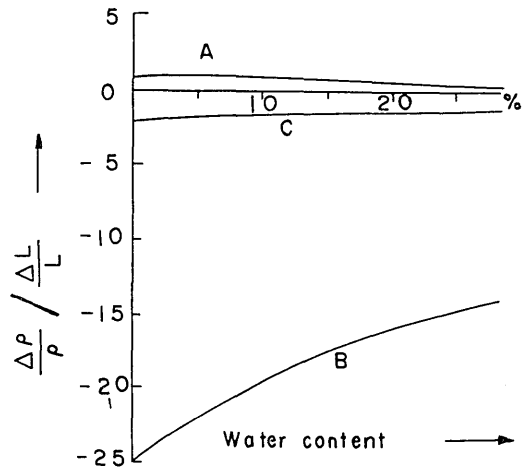

Fig. 17. Changes in $\frac{\Delta\rho}{\rho}/\frac{\Delta L}{L}$ with water content for the three models.

meters as before are calculated and shown in Fig. 17. σ is taken as 0.25 in the calculation. ρ means the apparent resistivity, so that $\frac{d\rho}{\rho}=-\frac{d\sigma_A}{\sigma_A}$.

---

75. 岩石変形と電気伝導度変化 (第二報)

(堆積岩についての室内実験)

地震研究所　山　崎　良　雄

第一報で岩石の歪と，電気伝導度，すなわち比抵抗の変化とについてのべた．とくに油壺の火山礫凝灰岩 (Lapilli tuff) では歪と比抵抗変化との比，$\frac{\Delta\rho}{\rho}\Big/\frac{\Delta L}{L}$ は 10^2～10^3 にもなることがあきらかになつた．

しかしこのときには岩石に加える圧力も，かんたんに変えることが出来ず，また実験の回数もすくなかつた．

今回はこれらのことを，たしかめるために，ブリッジ法の測定精度をたかめ，0～150 kg/cm² の油圧試験機を使用して，前回にもちいたとおなじ三種類の堆積岩について圧力試験をおこない，数多くの実験からつぎのような結果をえた．

火山礫凝灰岩では乾いたときには，$\frac{\Delta\rho}{\rho}\Big/\frac{\Delta L}{L}$ は 400，しめつてきて含水率 $w=18\%$ では 250，おなじく $w=25\%$ になると，25 と水分が岩石のなかに多くなつてくると，比抵抗の変化値 $\Delta\rho$，と $\frac{\Delta\rho}{\rho}\Big/\frac{\Delta L}{L}$ は小さくなつてくる．

油壺の凝灰質砂岩 (Tuffaceous sandstone) では $w=9.5\%$ のとき，$\frac{\Delta\rho}{\rho}\Big/\frac{\Delta L}{L}$ は 30，大谷の軽石凝灰岩 (Pumice tuff) では $w=5.6\%$ のとき，$\frac{\Delta\rho}{\rho}\Big/\frac{\Delta L}{L}$ は 18，と岩石の圧縮歪にたいする比抵抗変化との比は，二つとも火山礫凝灰岩にくらべて小さい．

岩石に圧力をかけると，いずれの堆積岩でも比抵抗の値は小さくなる．

岩石試料に圧力をかけた方向の歪，$\frac{\Delta L}{L}$ と $\frac{\Delta\rho}{\rho}\Big/\frac{\Delta L}{L}$ との関係は，火山礫凝灰岩では，$\frac{\Delta L}{L}$ の小さいときには第一報とおなじように，数百倍以上になり，$\frac{\Delta L}{L}$ が大きくなつてくると，$\frac{\Delta\rho}{\rho}\Big/\frac{\Delta L}{L}$ は小さくなつてくる．

軽石凝灰岩，凝灰質砂岩，の二つとも $\frac{\Delta L}{L}$，w，などに関係なく $\frac{\Delta\rho}{\rho}\Big/\frac{\Delta L}{L}$ はほとんど変わらない．

このちがいは第一報のなかで岩石を分類して名づけたとおり，A 型，O 型，という岩石の電気伝導のしかたの，ちがいによるものと考えられる．以上のことから，A 型の火山礫凝灰岩では 10^{-4} ぐらい，またはそれ以下の小さい歪が岩石にかかると，$\frac{\Delta\rho}{\rho}\Big/\frac{\Delta L}{L}$ は w の小さいときには数百倍以上にもなり，w が大きくなるにしたがつて小さくなつてくる．O 型の岩石では $\frac{\Delta\rho}{\rho}\Big/\frac{\Delta L}{L}$ は w に関係なくほとんど一定である．